Interactions between ultrasound stimulated microbubbles and fibrin clots

Christopher Acconcia,[1,2] Ben Y. C. Leung,[2] Kullervo Hynynen,[1,2] and David E. Goertz[1,2]
[1]*Department of Medical Biophysics, University of Toronto, Toronto M5S 1A1, Canada*
[2]*Sunnybrook Research Institute, 2075 Bayview Avenue, Toronto M4N 3M5, Canada*

(Received 24 June 2013; accepted 9 July 2013; published online 29 July 2013)

While it is well established that ultrasound stimulated microbubbles (USMBs) can potentiate blood clot lysis, the mechanisms are not well understood. Here we examine the interaction between USMBs and fibrin clots, which are comprised of fibrin networks that maintain the mechanical integrity of blood clots. High speed camera observations demonstrated that USMBs can penetrate fibrin clots. Two-photon microscopy revealed that penetrating bubbles can leave behind patent "tunnels" along their paths and that fluid can be transported into the clots. Finally, it is observed that primary radiation forces associated with USMBs can induce local deformation and macroscopic translation of clot boundaries. © *2013 AIP Publishing LLC*. [http://dx.doi.org/10.1063/1.4816750]

Over the past several decades, a range of ultrasound based approaches have been investigated to promote the degradation of blood clots.[1–3] Such "sonothrombolysis" techniques have potential clinical applications in the treatment of myocardial infarctions, peripheral vascular disease, and acute ischemic stroke, where the challenge of resolving thrombotic occlusions to restore blood flow in large vessels is a high clinical priority that is poorly addressed by current methods.[4] One of the more promising techniques is to employ ultrasound stimulated microbubbles (USMBs), which are currently in clinical use as diagnostic contrast agents. Despite a considerable body of work encompassing *in vitro*,[5–10] preclinical,[11–13] and initial clinical studies,[14,15] there remains uncertainty about the specific mechanisms by which USMBs achieve thrombolytic effects, either on their own or in conjunction with lytic enzymes (e.g., tissue plasminogen activator, or tPa). Histologic analyses of treated thrombus have shown that USMBs can enhance the penetration of lytic enzymes into clots.[8] It has been proposed that shear stresses arising from microstreaming or the occurrence of jets in the vicinity of bubbles oscillating adjacent to clots may act to mechanically cleave fragments from the clot surface. Fluid microdynamics around oscillating microbubbles (MBs) has also been hypothesized to contribute to mixing lytic agents at the clot boundary and thereby enhancing their thrombolytic effects. These heuristic mechanistic hypotheses stem in large part from what is known of the general behavior of acoustically stimulated bubbles adjacent to solid boundaries. Blood clots are, however, complex porous viscoelastic media comprised of platelets and red blood cells, which are enmeshed in a fibrin network that provides their mechanical stability. At present, there is an absence of direct evidence at a microscale about how microbubbles interact with the boundaries of clots, which is an impediment to furthering the development of exposure schemes and tailored microbubble agents to optimize treatment efficacy.

In this study, we investigate the interaction between USMBs and fibrin clots with a view to gaining basic mechanistic insights into the process of microbubble mediated sonothrombolysis. Fibrin clots are formed from purified fibrinogen and do not contain formed blood elements (e.g., platelets and red blood cells). They have been used extensively in thrombolysis drug studies[16,17] as the fibrin networks that make up these clots are the primary mechanical stabilizer of whole blood clots and their degradation is the target of enzymatic medical therapies. Fibrin clots are also nearly optically transparent, a property that is exploited in the present study to assess USMB interactions with microscopy approaches. In particular, fast frame camera (10 kfps) imaging was used to examine the interaction of microbubbles (Definity^{TM}) with the boundaries of fibrin clots under exposure to pulsed (1 ms duration, 15% duty cycle) 1 MHz ultrasound. Two-photon microscopy was then employed to evaluate the potential for damage to the fibrin networks induced by microbubbles, as well as to assess potential for the uptake of fluorescent nanobeads as a marker for fluid transport. A detailed methodology description is provided in the supplementary material.[23]

With the fast frame camera, it was observed that microbubbles were pushed through the adjacent fluid to the clot surface under the influence of primary radiation forces, at which point they could induce boundary deflections and, depending on the pressure level, penetrate into the clot. While within a clot, it was frequently observed that separate transiting microbubbles were drawn together under the influence of secondary radiation force and coalesced into a larger bubble before proceeding further. An illustrative image sequence is shown in Figure 1 (video available online) for the 0.4 MPa exposure condition. A bubble brought to the clot surface induces repeated local indentation and recovery cycles of the boundary during the course of successive ultrasound bursts before penetrating and undergoing translation in the direction of ultrasound propagation. It then merges with another bubble (initially out of the optical focal plane) before resuming its penetration. Notably, the bubble persists between bursts (5 ms intervals), and it is capable of shedding daughter bubbles. This persistence is of interest not only because the bubble remains available for acting on the clot across multiple ultrasound bursts, but also because it is consistent with the bubble not having undergone inertial collapse. Stable, non-inertial cavitation has previously been indicated to produce higher levels of clots lysis.[8] When within the clots, microbubbles will be subject to the boundary conditions of a porous viscoelastic medium, and it has previously been shown that bubbles

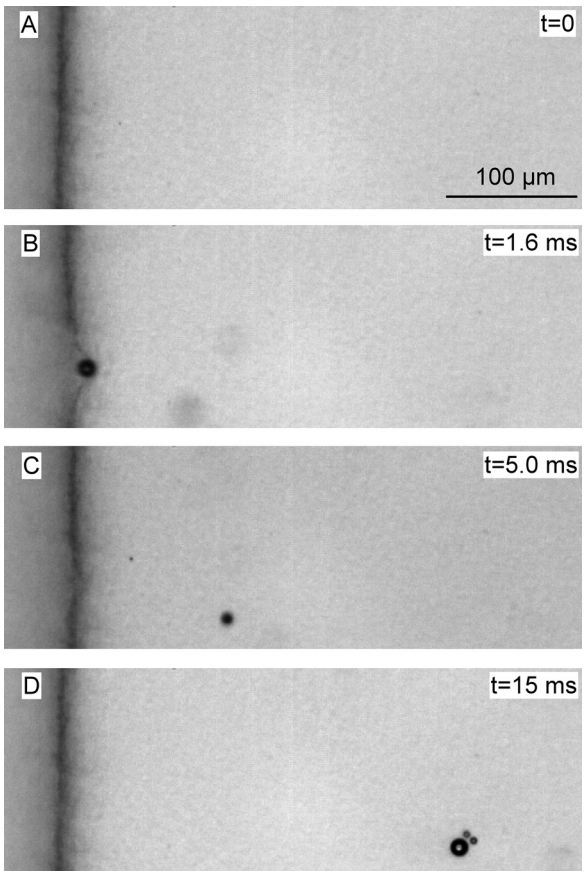

FIG. 1. An example sequence from a fast frame camera movie (10 kfps). (a) Prior to ultrasound exposure, this frame shows the fluid channel on the left and fibrin clot to the right. (b) A microbubble brought to the boundary induces repeated local deformations under primary radiation forces associated with successive bursts (0.4 MPa) before penetrating the clot and translating (c). After coalescing with another bubble its translation continues and an intact bubble, along with two daughter bubbles that it has shed, remains after the cessation of ultrasound (d). Ultrasound propagation direction is from left to right (enhanced online) [URL: http://dx.doi.org/10.1063/1.4816750.1].

situated within a confining viscoelastic medium will have a higher threshold for inertial cavitation,[18] though this has not previously been studied in fibrin clots.

In Figure 2, further example results are presented in the form of minimum intensity projection images (MIPs) derived from successive frames (movies online) in order to highlight the paths taken by bubbles during exposures (A:0.4 MPa; B: 0.8 MPa; C: 1.6 MPa). In the associated movie files, it can be seen again that bubbles are brought to the boundary, can induce deflections, penetrate, and transit through the clots. Penetrating bubbles translate predominately in the direction of ultrasound propagation, though the specific paths they negotiate will presumably be influenced to a degree by local variations of the fibrin network pore sizes and mechanical properties encountered. It is also evident that secondary radiation forces between nearby bubbles can alter their paths. One example of this is in Figure 2(a), where a bubble that has penetrated is subsequently drawn outwards to merge with a larger bubble outside the boundary. A second example is the prominent feature of Figure 2(c), where two penetrating bubbles translate towards each other and coalesce before continuing.

A total of $n = 6$ experiments per pressure condition were conducted. No bubble penetration events were observed at 0.2 MPa, but occurred for all pressures of 0.4 MPa and above. For bubbles that entered into the clots, the translation speed in the direction of ultrasound propagation increased with pressure. As a metric for this, the time to traverse 200 μm from the clot boundary in the direction of ultrasound propagation was estimated, where the total "on-time" of the bursts required for bubbles within the field of view was used. From 0.4–1.6 MPa, the results were 6 ± 2 ms, 0.42 ± 0.07 ms, and 0.38 ± 0.07 ms. The increases in translation speed with pressure is consistent with the bubbles experiencing higher levels of primary radiation forces,[19] as oscillation amplitudes are expected (not measured here) to increase with pressure.

These data appear to represent the first evidence of microbubble penetration into fibrin networks. Their entry and subsequent translation is likely enabled by the coupled effects of oscillations and the influence of primary radiation force, as has previously been postulated.[5,11] Secondary radiation force is also sufficient to overcome resistance of the fibrin network and translate separate bubbles together to coalesce. Outside the clot in fluid near the boundary, merging of bubbles was also observed. Indeed, it can be expected that the effects of secondary radiation forces near the boundary may be more prominent than in free solution as bubbles within the channel fluid are translated to the boundary this will increase their concentration and therefore reduce inter-bubble spacing. Such merging will increase the bubble sizes relative to those present within the native microbubble agent. While a wide range of bubble path widths were evident, it should be noted that due to the exposure duration of the camera (0.1 ms; far longer than an oscillation cycle), estimates of bubble sizes based on their dimensions in the images will reflect a time averaged diameter during oscillations. This, coupled with the frequent presence of bubbles out of the optical plane of focus compromise the ability to perform a quantitative analysis of bubble path widths.

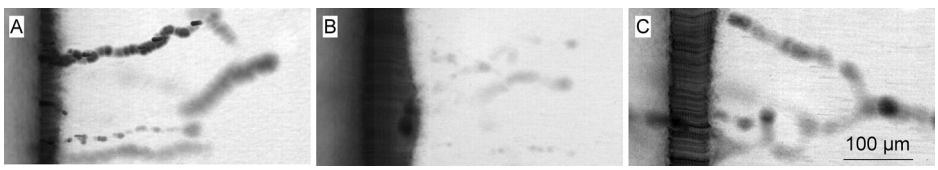

FIG. 2. Representative minimum intensity projection images derived from data acquired during the course of exposures at 0.4 (a), 0.8 (b), and 1.6 (c) MPa. MIPs were generated over 20 bursts in (a) and over a single burst in (b) and (c). Aside from the boundary deflection manifesting as the dark vertical band, a prominent feature in panel (c) is the path of two bubbles that enter the clot (ultrasound propagates from left to right), are drawn together and then proceed to the right, eventually exiting from the field of view (enhanced online) [URL: http://dx.doi.org/10.1063/1.4816750.2] [URL: http://dx.doi.org/10.1063/1.4816750.3] [URL: http://dx.doi.org/10.1063/1.4816750.4].

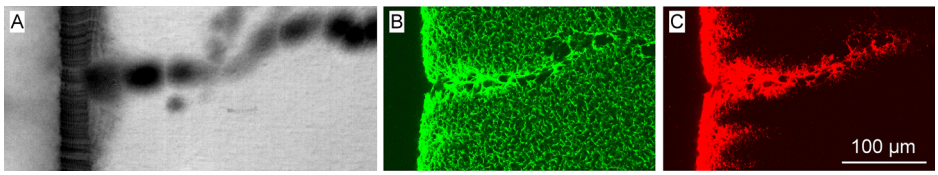

FIG. 3. Example co-registered MIP (a), two-photon fibrin network (b) and fluorescence nanobead (c) images (acquired for a 1.6 MPa exposure case). The prominent bubble path evident in the MIP image (a) is associated with generating a patent tunnel in the fibrin network (b), along which the uptake of fluorescent beads has occurred (c) (enhanced online) [URL: http://dx.doi.org/10.1063/1.4816750.5] [URL: http://dx.doi.org/10.1063/1.4816750.6] [URL: http://dx.doi.org/10.1063/1.4816750.7] [URL: http://dx.doi.org/10.1063/1.4816750.8].

A central question relevant to therapeutic applications is if penetrating bubbles are inducing damage to the fibrin network, which was assessed using 3D two-photon imaging of the fibrin networks following ultrasound exposures. An example MIP and its corresponding co-registered fibrin network image is shown in Figures 3(a) and 3(b), respectively. Along the path taken by the bubble, there is clear evidence of fibrin network damage, in the form of a patent tunnel remaining after its passage. These results indicate that the oscillations of translating bubbles, coupled with primary radiation forces, are sufficient to induce irreversible local structural damage to the fibrin network. In all cases where fibrin network tunnels were observed in regions coinciding with the co-registered optical field of view, there was a corresponding bubble path present on the MIP images. The presence of such network disruption was not observed at 0.2 MPa (no penetrating bubbles) but was in all exposures of 0.4 MPa and above. An analysis of the 3D two-photon data within the −3 dB beam widths of the exposed clot regions (1.6 mm laterally; depth range 0.2 mm) indicated there were an average of 2.6, 1.0, and 7.7 tunnels present in each clot for the cases of 0.4, 0.8, and 1.6 MPa, respectively. The number of tunnels present in the 0.8 MPa case was significantly lower than in the 0.4 ($p < 0.05$) and 1.6 MPa ($p < 0.00001$) cases. The reason for this will be the subject of future investigation, but one factor may be possible differences in the sizes of bubbles at the boundary due to different levels of secondary radiation force driven coalescence. This would in turn influence their resonant frequency, the level of primary radiation force experienced and their size relative to the dimensions of the fibrin network pores—all factors that may impact their ability to enter into the clot and induce damage.

A further therapeutically relevant question is if penetrating bubbles can promote the transport of liquids from the surrounding medium into the clots. Fluorescence imaging of the nanobeads post-sonication revealed that during these penetration events bubbles could transport with them nanobeads present in the channel fluid. Evidence of this is shown in Figure 3(c) (same scale as in Figures 3(a) and 3(b)) and its associated movie (a rotating 3D rendering of this tunnel is also provided online). The presence of nanobeads along the disrupted network bubble paths described above was observed in 23, 20, and 43% of cases for the 0.4, 0.8, and 1.6 MPa cases, respectively. These data therefore indicate that penetrating bubbles may be one means by which USMBs could enhance the uptake of enzymes into clots.

An analysis of the boundary displacements is shown in Figure 4. Panels (a)–(c) display examples of boundary displacements as a function of time for the cases of 0.4, 0.8, and 1.6 MPa, respectively. At earlier time points, displacements take the form of local deformations associated with the presence of individual bubbles impinging upon the boundary, which is followed by a period where there is a more homogeneous macroscopic boundary translation. The latter may be associated with either the cumulative effect of multiple bubbles, some of which may be out of the optical focal plane, or possibly due to a more spatially diffuse force pattern induced by bubbles that are translating within the fibrin network. In Figure 4(d), the mean boundary displacements are plotted as a function of time, beginning with the onset of the first

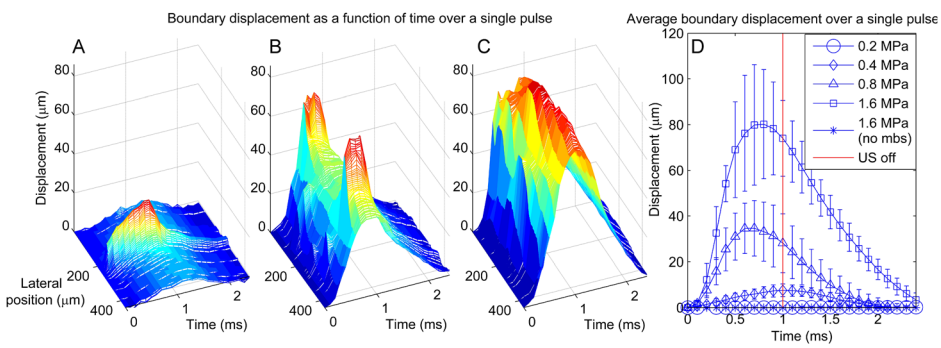

FIG. 4. Representative examples of boundary displacements in response to a single ultrasound burst as a function of time at pressures of 0.4 (a), 0.8 (b), and 1.6 MPa (c). Displacements (vertical axis) in the direction of ultrasound propagation are shown, where the "yposition" indicates position along the horizontal axis of the clot. These data show features of local indentations associated with individual bubbles at the boundary, along with a more macroscopic translation of the interface. In panel (d), the time course of the averaged boundary displacement is shown. The peak displacement increases with pressure, with the boundaries returning to their resting position over <2 ms after the bursts end. At 0.2 MPa, there is no detectible displacement, and in the case of no microbubbles being present, displacements are not detectible at any pressure.

transmitted ultrasound burst. The peak displacement level increases with pressure, as would be expected with pressure dependant increases in primary radiation forces. For the 0.2 MPa case, it is not detectible, and by 1.6 MPa the peak displacement reaches $80 \pm 24\,\mu$m. In the absence of microbubbles, no boundary displacement is measureable. It is of interest to note that ultrasound on its own is capable of producing tissue (and clot) displacements, to an extent that is related to the exposure intensity and the absorptive and mechanical properties of the tissue. Indeed, it has been shown that the displacements induced in clots by high intensity focused ultrasound produce strains across the ultrasound beam that can cause irreversible fibrin network pore widening to an extent that permeability to lytic enzymes is enhanced.[20] However, previous measurements of whole blood clot displacements in the absence of microbubbles indicate that for the pressure levels employed here, more readily achievable in transcranial ultrasound, clot displacement estimates would be on the order of only tens of nm.[21] The results of the present study indicate that the presence of microbubbles can induce displacements of fibrin clot boundaries to be on the order of tens of microns, which approaches levels previously observed in the absence of microbubbles at high ultrasound intensities.[21] Separate from this, it is recognized that localized oscillatory forcing loads that result in a cyclical deformation of the boundary of saturated porous viscoelastic media, as observed here at 0.4 MPa (e.g., Figure 1), can result in fluid transport within the poroelastic medium.[22] This appears not to have been previously investigated in the context of clots, but may warrant investigation as a possible mechanism for USMB potentiated lytic agent uptake.

This paper has presented the development of and initial results for an experimental approach designed to gain insight into the interactions between USMBs and fibrin clots. The study has a number of limitations that warrant comment. Foremost is that fibrin clots, while they are comprised of a fibrin network that is the primary stabilizing constituent of whole blood clots and are a well established model in thrombolytic studies, lack red blood cells and platelets. As such, it can be expected that there will be differences between the results obtained here and those that occur within whole blood clots. The presence of blood cells would likely alter their paths and limit their penetration depth relative to what has been reported here. Further, we have focused on examining the effects of a discrete number of ultrasound bursts (20) with a view to gaining mechanistic insight into the interaction between USMBs and fibrin networks, whereas previous sonothrombolysis studies expose the clots to USMBs for prolonged periods (minutes to tens of minutes) and therefore capture more advanced erosion effects (e.g., clot mass loss) arising from a large number of USMB-clot interaction events.[5] Experiments were not conducted in the presence of fibrinolytic enzymes, which would be expected to result in a more pronounced degradation of the fibrin networks. Finally, while the fast frame camera at10 kfps enabled examination of longer timescale interactions between USMBs and the clots, it precluded accurate bubble size measurements. These are currently being investigated with individual microbubble experiments, wherein it will also be of interest to examine the effects of different pulsing approaches and non-orthogonal beam/boundary orientations. Within these constraints, the results have provided a number of basic insights: bubbles can deform clot boundaries, penetrate and enhance the transport of fluids into fibrin clots, and locally disrupt the structure of fibrin networks leaving behind patent tunnels. Complex microbubble behavior is indicated, involving the interplay between primary and secondary radiation forces and their interaction with a confining matrix. An improved understanding of the behavior of microbubbles not just within free solution but adjacent to and confined within the poroelastic medium that makes up clots will be important in moving towards the development of improved agent design and exposure schemes to promote thrombolysis.

The authors would like to thank Harry Easton for his design insights and skillful machining of the chamber used in this work. The authors would also like to thank Brandon Helfield for the many helpful insights gained in our interactions. This work was financially supported by the Natural Sciences and Engineering Research Council of Canada.

[1]S. Pfaffenberger, B. Devcic-kuhar, S. P. Kastl, K. Huber, G. Maurer, J. Wojta, and M. Gottsauner-Wolf, Thromb. Haemostasis **94**, 26 (2005).
[2]A. V. Alexandrov, C. A. Molina, J. C. Grotta, Z. Garami, S. R. Ford, J. Alvarez-Sabin, J. Montaner, M. Saqqur, A. M. Demchuk, L. A. Moyé, M. D. Hill, and A. W. Wojner, N. Engl. J. Med. **351**, 2170 (2004).
[3]R. Medel, R. W. Crowley, M. S. McKisic, A. S. Dumont, and N. F. Kassell, Neurosurgery **65**, 979 (2009).
[4]The National Institute of Neurological Disorders and Stroke rt-PA Stroke Study Group, N. Engl. J. Med. **333**, 1581 (1995).
[5]B. Petit, E. Gaud, D. Colevret, M. Arditi, F. Yan, F. Tranquart, and E. Allémann, Ultrasound Med. Biol. **38**, 1222 (2012).
[6]F. Xie, E. C. Everbach, S. Gao, L. K. Drvol, W. T. Shi, F. Vignon, J. E. Powers, J. Lof, and T. R. Porter, Ultrasound Med. Biol. **37**, 280 (2011).
[7]T. R. Porter, D. Kricsfeld, J. Lof, E. C. Everbach, and F. Xie, J. Ultrasound Med. **20**, 1313 (2001).
[8]S. Datta, C.-C. Coussios, A. Y. Ammi, T. D. Mast, G. M. De Courten-Myers, and C. K. Holland, Ultrasound Med. Biol. **34**, 1421 (2008).
[9]K. E. Hitchcock and C. K. Holland, Stroke **41**, S50 (2010).
[10]K. Tachibana and S. Tachibana, Circulation **92**, 1148 (1995).
[11]Y. Birnbaum, H. Luo, T. Nagai, M. C. Fishbein, T. M. S. Li, D. Kricsfeld, T. R. Porter, and R. J. Siegel, Circulation **97**, 130 (1998).
[12]W. C. Culp, T. R. Porter, J. Lowery, F. Xie, P. K. Roberson, and L. Marky, Stroke **35**, 2407 (2004).
[13]A. T. Brown, R. Flores, E. Hamilton, P. K. Roberson, M. J. Borrelli, and W. C. Culp, Invest. Radiol. **46**, 202 (2011).
[14]C. A. Molina, A. D. Barreto, G. Tsivgoulis, P. Sierzenski, M. D. Malkoff, M. Rubiera, N. Gonzales, R. Mikulik, G. Pate, J. Ostrem, W. Singleton, G. Manvelian, E. C. Unger, J. C. Grotta, P. D. Schellinger, and A. V. Alexandrov, Ann. Neurol. **66**, 28 (2009).
[15]C. A. Molina, M. Ribo, M. Rubiera, J. Montaner, E. Santamarina, R. Delgado-Mederos, J. F. Arenillas, R. Huertas, F. Purroy, P. Delgado, and J. Alvarez-Sabín, Stroke **37**, 425 (2006).
[16]J.-P. Collet, J. L. Moen, Y. I. Veklich, O. V. Gorkun, S. T. Lord, G. Montalescot, and J. W. Weisel, Blood **106**, 3824 (2005).
[17]D. A. Meh, M. W. Mosesson, J. P. Diorio, K. R. Siebenlist, I. Hernandez, D. L. Amrani, and L. Stojanovich, Blood Coagul Fibrinolysis **12**, 627 (2001).
[18]X. Yang and C. C. Church, ARLO **6**, 151 (2005).
[19]P. A. Dayton, J. S. Allen, and K. W. Ferrara, J. Acoust. Soc. Am. **112**, 2183 (2002).
[20]G. Jones, F. Hunter, H. A. Hancock, A. Kapoor, M. J. Stone, B. J. Wood, J. Xie, M. R. Dreher, and V. Frenkel, IEEE Trans Biomed. Eng. **57**, 33 (2010).
[21]C. C. Wright, K. Hynynen, and D. E. Goertz, IEEE Trans. Biomed. Eng. **59**, 842 (2012).
[22]W.-C. Lin, K. R. Shull, C.-Y. Hui, and Y.-Y. Lin, J. Chem. Phys. **127**, 094906 (2007).
[23]See supplementary material at http://dx.doi.org/10.1063/1.4816750 for detailed description of the experimental apparatus, procedure and clot preparation.